Accepted Manuscript

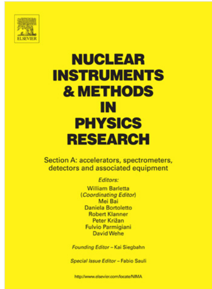

Deuterated stilbene (stilbene-d_{12}): An improved detector for fast neutrons

F.D. Becchetti, R.O. Torres-Isea, A. Di Fulvio, S.A. Pozzi, J. Nattress,
I. Jovanovic, M. Febbraro, N. Zaitseva, L. Carman

PII: S0168-9002(18)30965-3
DOI: https://doi.org/10.1016/j.nima.2018.08.021
Reference: NIMA 61062

To appear in: *Nuclear Inst. and Methods in Physics Research, A*

Received date : 14 March 2018; Revised date : 1 August 2018;
Accepted date : 7 August 2018

Please cite this article as: F.D. Becchetti, et al., Deuterated stilbene (stilbene-d_{12}): An improved detector for fast neutrons, *Nuclear Inst. and Methods in Physics Research, A* (2018), https://doi.org/10.1016/j.nima.2018.08.021

Deuterated Stilbene (stilbene-d_{12}): An Improved Detector for Fast Neutrons

8/23/2018

F.D.Becchetti and R.O. Torres-Isea
Department of Physics, University of Michigan, Ann Arbor MI 48109, United States

A. Di Fulvio, S.A.Pozzi, J. Nattress and I. Jovanovic
Department of Nuclear Engineering and Radiological Sciences, University of Michigan, Ann Arbor MI 48109, United States

M. Febbraro
Oak Ridge National Laboratory, Oak Ridge TN 37830, United States

N. Zaitseva and L. Carman, Lawrence Livermore National Laboratory, Livermore, CA 94551, United States

Abstract

We have developed and evaluated two prototype fast neutron deuterated-stilbene scintillators. The largest scintillator is hexagonal in shape with volume 32 cm^3, comprised of deuterated crystalline trans-stilbene (stilbene-d_{12}). These samples were grown using a solution-based crystal growing method developed at Lawrence Livermore Laboratory to grow conventional ^1H-based stilbene scintillator crystals. The stilbene-d_{12} prototype detectors show excellent neutron/gamma discrimination, noticeably better than ^1H-stilbene, and appear to have less asymmetry in the response to neutrons incident from different directions. Like other deuterated scintillators, the stilbene-d_{12} detectors in many applications can provide incident neutron energy spectra, without time of flight, by suitably unfolding the neutron light-output spectra.

1. Introduction

The ideal fast neutron detector would: a) have excellent neutron-gamma pulse-shape discrimination (PSD), b) provide useable neutron energy information i.e. spectra, without need for time of flight (ToF), c) have excellent fast timing characteristics, d) be solid-state, e) be non-hygroscopic, f) have light emission matched to photo-multipliers (PMTs) or silicon photo-detectors, g) have good detection efficiency and resolution, h) be non-flammable and relatively safe to handle, i) be compatible with most optical greases and optical epoxies, and j) be available at low cost in large volumes. Except for the latter (size and cost), we believe the neutron detector we have recently developed, which is based on deuterated trans-stilbene (stilbene-d_{12}), satisfies these requirements. The basic characteristics of two prototype stilbene-d_{12} detectors, the largest 32 cm^3, a size practical for many nuclear reaction measurements, are compared with those of conventional i.e. ^1H-based stilbene detectors, and confirms the above. This paper presents the initial set of measurements. The growth of the crystals and their optical properties are described in detail in [1]. Likewise additional details on the response, pulse-shape discrimination, linearity, and other properties of the detectors, including additional measurements of neutron spectra will be reported in [2].

2. Development and evaluation: prototype detectors

The synthesis of high-quality ^{1}H-based, i.e. conventional trans-stilbene crystals for use as neutron detectors has been developed at Lawrence Livermore National Laboratory (LLNL) using a solution-growth method [1,3]. The basic starting compound is ^{1}H-based styrene, which also is available in a deuterated version [4]. Hence the possibility to grow deuterated-stilbene crystals was deemed feasible and pursued as a joint project between the University of Michigan (UM), Oak Ridge National Laboratory (ORNL) and LLNL, with the deuterated material supplied by UM [5]. As demonstrated by Brooks, et al. [6,7], using deuterated anthracene and later deuterated organic liquid benzene-based scintillators (NE230/BC537), replacing the hydrogen in these scintillators with deuterium produces a recoil-deuteron spectrum in the scintillator light output (L) that has broad peaks corresponding to the incident neutron energy with E_d=8/9 E_n [5,6,7]. This approach is in contrast to ^{1}H-based scintillators that have a rather non-distinct light spectrum without prominent peaks. Recent developments in digitized-pulse data acquisition, along with efficient, fast computer spectral unfolding and techniques for measuring accurate detector response functions over a range of neutron energies has led to new applications using deuterated liquid organic scintillators [5]. This includes nuclear reaction studies [8,9,10] and applications in nuclear counter terrorism and nuclear non-proliferation [11]. However, while deuterated liquid scintillators have adequate PSD for most measurements, their PSD is often inadequate at low incident neutron energies (e.g. E_n<1 MeV) or incident neutron energies > 10 MeV where for the latter scintillator deuteron break-up can be significant and results in protons being detected along with recoil deuterons [5,6]. At even higher neutron energies other nuclear reactions in the scintillators can greatly complicate the PSD [12] and the non- linearity in the response can be an issue [13-16]. As noted in the introduction, an improved scintillator material would have excellent PSD over a wide range of incident neutron energies. This would permit measurements at lower neutron energies (few MeV) as well as higher energies (tens of MeV) where deuteron breakup protons and other nuclear reactions in the scintillator must be identified and removed, while still providing information on the incident neutron energy via the recoil deuteron. However, liquid scintillators require a sealed cell and many of the liquids used are toxic and flammable. A safe, non-hygroscopic crystalline detector would be advantageous for many applications.

3. Scintillator properties

The properties of ^{1}H- and ^{2}H-stilbene (the latter stilbene-d_{12}) compared with a commonly used ^{2}H-based liquid scintillator (benzene-d_6; NE230, BC537 and EJ315) are shown in Table 1. The emission spectra are similar (blue fluorescence) and well matched to most photo-detectors, but stilbene has a higher light output. (The recently-developed EJ301D liquid scintillator, xylene-d_{10}, also has several advantages relative to benzene-d_6 [17,18]). The synthesis of both ^{1}H and ^{2}H stilbene begins with the appropriate styrene compound (normal or deuterated), along with suitable catalysts and solvents (normal or deuterated) to allow for uniform crystal growth in solution producing a crystal with good optical properties [1,3,5,19]. Unfortunately, the present availability of deuterated styrene is limited and the amounts used in this project were obtained via small, in-stock commercial quantities [4]. This made the detectors more expensive (ca. \$200/cm^3) than possible if bulk material would have been available or if such material could have been custom synthesized in a single batch. Nonetheless, in many applications the detectors may not be the major cost of the experimental apparatus, and the cost could be justified given their efficiency to make fast neutron energy measurements with excellent n/γ separation without need to use the time-of-flight technique [5].

4. Detector evaluation: ^{252}Cf Fission-source PSD and spectra

Two stilbene-d_{12} (trans-stilbene) crystals were evaluated: a small crystal ca. 1.5 cm thick, 11 cm^3 in volume, among the first ever produced [5], and a second crystal, of similar hexagonal shape (Fig.1) ca. 3.55 cm thick, and 32 cm^3 in volume, a size practical for many types of neutron measurements (see below). A companion ^{1}H-stilbene crystal was also grown at the same time (Fig. 1) to permit direct comparison with the 32 cm^3 stilbene-d_{12} crystal. Initial evaluation of the smaller crystal has been reported previously [5]. The 32 cm^3 detector crystals were covered with teflon tape as a reflector, mounted with Eljen EJ-550 silicon-based optical grease to 51 mm dia. ET 9241B PMTs or equivalent, and held in place with tight-fitting thin black vinyl caps and black electrical tape. Mu-metal shields covered the PMT, extending several cm beyond the photo cathode to negate the effect of the Earth's magnetic field. The PMTs were selected where possible to have matched gains to within a few %, so they could be operated at their recommended high voltages (HV). However the latter HV can produce PMT signals beyond the input voltage range of the high-speed CAEN pulse digitizers used to digitize the PMT anode signals (for most measurements a CAEN DT5730 digitizer, 500 MS/s, 2 nsec sampling rate,14 bits). Therefore, precision attenuators as needed were used on the PMT signals to match the input voltage range of the digitizer. This approach allowed the PMTs to be operated at their optimal HV bias for many of the measurements and thus yielded data with good signal-to-noise characteristics and fast timing (i.e. minimal transit-time spread in the PMT).

After initial testing at LLNL [1], the performance of the 32 cm^3 prototype detectors were further evaluated using various ^{252}Cf fission neutron sources as well as mono-energetic neutrons from DD and DT neutron generators (2.5 MeV and 14.1 MeV neutrons, respectively) at ORNL and UM. Calibration of the scintillator light spectra in terms of electron-equivalent energy units (keVee or MeVee) was done using various gamma sources but primarily ^{137}Cs and ^{22}Na where the Compton edge (per past measurements taken as ca. 80 % of the Compton spectrum maximum) was used for the calibration [11,20-22].

The PSD capability of the scintillator was evaluated using the charge integration (CI) method. The CI algorithm calculates the pulse integral over two regions: the first region, or "total" integral includes the entire digitized pulse, and the second region, or "tail" integral begins several nanoseconds after the pulse maximum and extending to the same time limit as the total integral. Good PSD performance was achieved for both the ^{1}H-stilbene and stilbene-d_{12}, with the tail integration beginning 22 nsec after the pulse maximum and ending after 344 nsec. The total pulse was integrated starting 4 ns before the maximum for a total integration time of 370 nsec, which is typical for stilbene measurements [1,3], but may miss some of the delayed light.

PSD and light spectra obtained with the 32 cm^3 stilbene-d_{12} detector using a ^{252}Cf source are shown in Figs. 2 and 3 and compared with those for the matching ^{1}H-stilbene detector. This result is consistent with what we observed with the smaller crystal [5], with the n-γ PSD separation for the former approximately 20 % better. This is due in part to the higher ionization track density, hence saturation, in the recoil deuteron path versus a recoil proton producing the scintillation light [5,13-16]. As with conventional stilbene [1], with suitable optimization of the digital PSD algorithm, it appears the lower threshold for neutron detection (e.g. PSD figure-of-merit >3) can be set below 20 keVee (electron-equivalent energy) and thus E_n< 200 keV [5,15]. This could prove critical in many applications including nuclear reaction measurements, especially those using exotic, radioactive nuclear beams, as well as nuclear security applications [5,20-22]. In particular, the energy information available from deuterated scintillators can be used to identify different types of fissionable, weapons-grade material [11,20]. As noted, in many cases the above features would help justify the higher fabrication cost of this type of detector.

5. Compton scattering measurement: Electron response and detector resolution

The direct response and resolution of the 32 cm^3 stilbene-d_{12} detector system (PMT with mounted crystal) to electrons was determined using Compton scattering of ^{137}Cs 0.662 MeV gamma rays entering sideways into the stilbene-d_{12} crystal. These were scattered by the stilbene-d_{12} into a NaI(Tl) gamma detector positioned at specific angles and set in coincidence with the recoil electron detected in the stilbene-d_{12} crystal [17]. The recoil electron energy spread due to the angular acceptance of the gamma ray detector and the emission and detection angle spread due to the gamma source and stilbene-d_{12} detector collimation was then calculated and unfolded in quadrature from the measured recoil electron energy spectrum (Fig. 4) to deduce the detector response (L) and resolution (δL/L) in electron-equivalent units (MeVee). Conventional analog nuclear (NIM) electronics and a multi-channel analyzer (MCA) were employed for the measurements with a precision NIM pulser used to determine and correct for any MCA offset [17]. The results for the stilbene-d_{12} detector resolution L< 1 MeVee are shown in Fig. 5. Additional resolution data were obtained from monoenergetic neutrons from DD (2.5 MeV) and DT (14.1 MeV) neutron generators (next section).

In addition to the coincident-electron Compton calibrations, the Compton edges from various gamma-source spectra (^{137}Cd,^{54}Mn,^{22}Na,^{60}Co) using again as a criterion 80% of the Compton gamma peak maximum were also determined. While these data overlap the Compton coincident-electron data below 600 keVee or so, a linear extrapolation of that data to higher energies underestimates the Compton edge data values. Data obtained using the digitizer CI method were somewhat more linear. However, the linearity can depend on several factors including pulse integration times, PMT HV, etc. [12-16] and will be discussed in more detail in [2].

If the detector resolution were primarily limited by the number of photons produced and then converted to photoelectrons at the PMT (hence proportional to L), we would then anticipate a statistical spread in L related to the number of photoelectrons produced and thus proportional to $L^{1/2}$. We then would expect a detector resolution δL/L proportional to $L^{-1/2}$. However, this is only partially correct as other factors obviously contribute to the resolution. In particular, the crystal geometry and size, the location of the neutron interaction, the presence of double scattering events, the possibility of escaping recoil deuterons, the uniformity of the reflective medium, the PMT and electronics noise, the non-proportionality of the photon production in the crystal [13,14], the linearity of the PMT, and other factors must be considered. It is found that most scintillator detector resolution data can be fit with an empirical equation of the form δL/L (%)=100 Sqrt [a+ b/L +c/L^2] where "a" represents the light collection efficiency from the scintillator to the PMT, "b" the statistical variation in the crystal photons produced and the subsequent PMT photoelectron production, i.e. the PMT conversion efficiency, and "c" represents the noise contributions from the PMT and electronics. Other factors (above) which may contribute are therefore also included in these empirical fitting parameters.

In Fig. 5 we display the δL/L (%) equation fit [16] to the reported detector resolution of a 7.6 cm dia. X 7.6 cm long commercial deuterated benzene scintillator assembly (EJ315). Based only on the number of photons produced in stilbene (90 % of anthracene, Table 1) and possibly detected, estimated to be about 4000 /MeVee at 500 KeVee, we would expect δL/L (%) due to the photon statistics in the crystal alone to be no better than about 4.5 % FWHM. However, both the commercial EJ315 detector [16] and our d-stilbene detectors exhibit 2-3 times that indicating major contributions from the other factors involved and in particular from the collection and conversion of the photons produced in the crystal to photoelectrons in the PMT as well as possible non-linear signal production in the crystal and PMT (above). It should be noted that our δL/L measurements are from direct Compton-electron coincidence measurements whereas those reported in [16] use a model-dependent method to extract the detector light resolution from normal Compton spectra.

As expected, the higher light output of stilbene (Table 1) results in an improved resolution at higher L values where photon and PMT photoelectron production statistics dominate. As an example, at 6.5 MeVee (14.1 MeV neutrons) even without an optimized crystal mounting cell and special high-efficiency PMT, we observe δL/L of about 8 % (see below) which is better than that of typical deuterated liquid detectors, although these are generally larger in size [5]. However, this limited detector light resolution does not preclude unfolding the light spectra and obtaining better resolution in the neutron energy spectra (to a few %) provided one has good statistics, low-noise electronics, good light collection, together with accurate detector response functions [16,18-21]. We plan to demonstrate this in the near future for the present and other stilbene-d_{12} detectors using in-beam nuclear reaction measurements [2,5,20].

6. Detector evaluation: DD and DT neutrons (E_n= 2.5 and 14.1 MeV)

The PSD and neutron light spectra (gated by PSD) of the 32 cm^3 detectors to 2.5 MeV and 14.1 MeV deuterons were measured at UM using commercial DD and DT neutron generators [ThermoFisher MP320(DD) and P211(DT)] with arrangements similar to that shown in Fig. 6. (Similar measurements done at ORNL were used to verify the UM measurements). Since the DD and DT generators produce neutrons over a wide range of angles, the room-return neutrons are a significant background and partially obscure the 2.5 MeV and 14.1 neutron groups. This measurement requires use of shadow bars to remove this background and observe the DD and DT neutron groups to better than 10 % accuracy. Thus, steel or composite neutron shadow bars, ca. 4 in. diameter, consisting of 12 inches of steel alone (DD measurements) or followed by 12 inches of polyethylene (DT measurements) were located between the neutron generator and the detectors in order to obtain the background due to scattering of room-return neutrons (Fig. 6). This primarily affects the lower energy portion of the spectra, which however is needed for accurate spectral unfolding. As expected [5], and in contrast to ^{1}H-stilbene, especially after background subtraction the stilbene-d_{12} light spectrum from the DD generator (2.5 MeV neutrons) displays a broad but distinct peak in both the PSD and the light spectra similar to those observed in deuterated liquid scintillators [5,15,16,20,21], corresponding to the incident neutron energy (Figs. 7 and 8),

As shown with other deuterated scintillators, this should then allow for the accurate unfolding of the light spectrum to deduce the incident neutron energy spectrum once the detector response functions are known [5,9,15,16,20,21] and room-return neutrons removed as needed. Fortunately, for many nuclear reaction studies the neutrons of interest are often preferentially emitted at forward angles and room-return neutrons are less of an issue [20,21]. Future measurements are planned to verify this and extract various (d,n) nuclear reaction spectra.

Similar spectra were obtained with 14.1 MeV neutrons from the DT generator using the composite steel and polyethylene shadow bars to remove room-return neutron background (Fig. 6). Again, owing to the larger ionization density for the recoil deuterons, the light output is noticeably lower than for the similar-size ^{1}H-stilbene detector, where the latter still has much less distinct features (Figs. 9,10). At this higher neutron energy there is some indication of scattered neutrons entering the detectors from the primary or adjacent shadow bar (Fig.1), which limited the accuracy of the background correction for the light spectra at the lowest energies. In addition, for 14.1 MeV incident neutrons the break-up of the deuterons in the scintillator also must be considered [5,12]. This effect is indicated in the corresponding PSD spectrum (Fig.9), where both recoil deuterons and break-up protons appear close together in PSD vs. L. Although the protons have lower energy than the deuterons, they produce a higher light output and hence can overlap with the deuterons in the light spectrum. However, owing to the excellent PSD of stilbene, here with a figure-of-merit, FOM, of 6 or more when optimized [3], the protons can then be separated from the recoil deuterons by suitable gating on the PSD spectrum (Figs. 9-11). In the present measurements, the PSD quality was limited by the sampling rate (2 nsec) of the digitizer, which is not optimal for the stilbene detectors evaluated as they have very fast rise time (<2 nsec) and fall time (< 4 nsec) when coupled to a fast PMT. Fortunately, the break-up protons and other ions produced in the scintillator, depending on the Q values for the nuclear reactions under study, may not necessarily interfere with the higher energy portion of the deuteron-recoil light output spectra. Nonetheless by careful PSD gating a clean deuteron-recoil light spectrum could be obtained yielding a very distinct peak corresponding to 14.1 MeV neutrons (Fig. 11). The resolution is approximately 8 % FWHM in L, which is close to that expected (5-8 % FWHM) from extrapolation of the data shown in Fig.5 using the semi-empirical relation previously given for $\delta L/L$ fitted to the d_{12}-stilbene data above 0.2 MeVee.

In experiments where low energy gamma rays can be an issue, one can enhance the n/γ PSD by using a thin lead sheet to attenuate the low-energy gamma rays with little attenuation of the neutrons. As noted, it appears to then be possible to cleanly separate neutrons to <20 keVee (i.e.< 200 keV neutrons, [15]). Likewise if short-path ToF is available, although not used to determine neutron energies, it can still be used to remove most of the prompt gamma rays associated with a nuclear process [20,21,23].

One advantage of even modest energy discrimination in an organic deuterated scintillator when they are used as part of a close-packed or segmented large neutron detector array, is the capability to eliminate scattered and hence much lower energy neutrons from adjacent detectors or segments via the scintillator light signal (Fig. 11).

7. Measurement of asymmetrical response

Conventional stilbene is known to have a noticeable asymmetry with respect to direction of the incident neutrons with respect to crystal orientation [19,24]. We studied this property in the smaller stilbene-d_{12} detector using 2.5 MeV neutrons from the DD generator (Fig.12). As seen in the figure, in contrast to ^{1}H-based conventional stilbene, there appears to be little asymmetry in the light output, at least for the crystal and angles tested. We note that the range of the recoil deuterons are much shorter (approximately ½, [12]) than the recoil protons of the same recoil energy in conventional stilbene. This may minimize any asymmetry effects in the response and warrants further study.

8. Neutron detection efficiency

The overall detection efficiency for ^{252}Cf fission neutrons was measured for neutrons above 23 keVee in light output (corresponding to approximately 230 keV neutron energy deposited) for the 32 cm^3 stilbene detectors using a calibrated ^{252}Cf source. It was determined to be 12.2 +/-0.6 % for the stilbene-d_{12} detector and 21.1+/- 1.1 % for the similar-size ^{1}H-stilbene detector. This result is comparable to the calculated efficiency for similar-size deuterated-liquid scintillators when coupled to modern PMTs. It reflects the differences in the n+d and n+p scattering cross sections over this energy range [3,4] and the difference in light output of the two scintillators (Fig.7). The MCNPX-PoliMi Monte-Carlo scintillator simulation code and related modules [25] are presently being modified to include the measured light output vs. neutron energy for deuterated stilbene. This code enhancement will permit calculations for the light spectra and detection efficiencies expected at higher neutron energies, for example as needed for nuclear reaction analyses [3,20-22].

9. Conclusions

Two samples of deuterated trans-stilbene (stilbene-d_{12}) crystals configured with fast PMTs as neutron detectors have been evaluated, the largest being 32 cm^3. These first samples exhibit excellent PSD (figure-of-merit, FOM [19]) , 6 or better for neutron energies 2-10 MeV. The small crystal tested exhibits little asymmetry in the light output, better than conventional stilbene. As expected, the stilbene-d_{12} scintillators produce light-output spectra with neutron energy information without need for ToF. As with conventional stilbene, these crystals are relatively safe to handle, are non-hygroscopic and appear well suited for many applications including nuclear reaction studies, nuclear security, and nuclear non-proliferation. This will be verified in additional experiments. The main issue at the moment is the high initial cost of the starting material (deuterated styrene) but hopefully this can soon be addressed and help make these improved fast-neutron detectors available at a more reasonable cost [27].

Recently, small samples of a glass scintillator have been developed and evaluated that show promise [28] for combined neutron and gamma detection, especially if they also can be made deuterated. While these samples, albeit small samples, have been shown to have better performance than normal stilbene e.g. better PSD, the present, large crystals of stilbene-d_{12} we have evaluated also have improved performance (FOM 6 or better) relative to conventional stilbene. In addition the stilbene-d_{12} can provide neutron energy information from the recoil deuteron spectrum producing the light spectrum, especially when the latter is suitably unfolded [5,20-22]

Acknowledgements

We thank our colleagues and the referees for useful comments and suggestions. This work was supported in part by NSF Grant PHY 14-01242. This work was also supported by the U.S. Department of Homeland Security under Grant Awards No. 2014-DN-077- ARI078-02 and 2015-DN-077-ARI096. The research of J. Natress was performed under appointment to the Nuclear Nonproliferation International Safeguards Fellowship Program sponsored by the National Nuclear Security Administration's Office of International Safeguards (NA-241).Additional support provided by the Department of Energy and in particular, this material is based upon work supported by the U.S. Department of Energy, Office of Science, Office of Nuclear Physics, and NA-22 office, under Award Number DE-AC05-00OR22725 and Contract Number DE-AC52-07NA27344. Support also provided by the Consortium for Verification Technology under Department of Energy National Nuclear Security Administration award number DE-NA 0002534.

Table 1. Comparison of ^{1}H-, ^{2}H-based stilbene scintillators with ^{2}H-benzene liquid scintillator (benzene-d_6, EJ315)

	Conventional stilbene	^{2}H-stilbene (stilbene-d_{12})	^{2}H-benzene (benzene-d_6)[b]
Chemical formula	$C_{14}H_{12}$	$C_{14}D_{12}$	C_6D_6
Density (g/cm^3)	1.16	1.24 [a]	0.95
Melting pt. (^{0}C)	124	est. 124 [a]	n.a.
Crystal type	biaxial monoclinic	biaxial monoclinic	n.a.
Max. emmission (nm)	380 (blue)	est. 380[a]	425 [b]
Light output (% anthracene)	90 [c]	90 [a] [c]	60 [b]
Index of refraction (590 nm)	1.70-1.84	1.70-1.84[a]	1.50 [b]
Fast decay component (nsec)	<4	<4 [a]	3.5 [b]

a) Assumed to be similar to conventional [1,3,19] stilbene.
b) Eljen, inc. data for EJ315 [26]; benzene-d_6 liquid has a fluor added.
c) Estimated. Includes only portion of light matched to a typical PMT response i.e. excludes the red portion of the anthracene scintillation light.

References

1) M.L. Carman, A.M. Glenn, Andrew N. Mabe,F.F. Becchetti, S.A. Payne, N.P.Zaitseva, Solution growth of a deuterated trans -stilbene crystal for fast neutron detection, Journal of Crystal Growth (in press) https://doi.org/10.1016/j.jcrysgro.2018.05.021

2) Angela Di Fulvio, et al. Characterization of Deuterated-stilbene (stilbene-d12) for Neutron Spectroscopy, Proc. SORMA XVII Conference, Ann Arbor MI (2018)

3) Natalia Zaitseva , Andrew Glenn, Leslie Carman, H. Paul Martinez, Robert Hatarik, Helmut Klapper, and Stephen Payne, Scintillation properties of solution-grown trans-stilbene single crystals, Nucl. Instrum. Methods Phys. Res. A **789** (2015) 8–15

4) Sigma-Aldrich, St.Louis, MO USA

5) F.D. Becchetti, R.S. Raymond, R.O. Torres-Isea, A. Di Fulvio , S.D. Clarke, S.A. Pozzi, M. Febbraro, Recent developments in deuterated scintillators for neutron measurements at low-energy accelerators, Nucl. Instrum. Methods in Phys. Res. A **874** (2017) 72-78

6) F.D. Brooks, W.A. Cilliers, B.R.S. Simson, F.D. Smit, M.S. Allie, D.T.L. Jones, W.R.McMurray, J.V. Pilcher, Deuterated anthracene spectrometer for 5-30MeV neutrons, Nucl. Instrum. Methods Phys. Res. A **270** (1988) 149–156

7) F.D. Brooks, P.M. Lister, J.M. Nelson, K.S. Dhuga, Vector analyzing powers for the 12C(d,n)13N, 9Be(d,n)10B, and 28Si(d,n)29P reactions, AIP Conf. Proc. **69** (1981) 656–658

8) D.A. Roberts, et al., Neutron decay from the isobaric analog state in 120Sb populated in 120Sn(3He,t)120Sb at E(3He) = 200 MeV, Phys. Rev.C **52** (1995) 1361–1367

9) M. Ojaruega, F.D. Becchetti, A.N. Villano, H. Jiang, R.O. Torres-Isea, J.J. Kolata, A. Roberts, C.C. Lawrence, Evaluation of large deuterated scintillators for fast neutron detection (E=0.5-20 MeV) using the D(d,n)3He,13C(d, n) and 27Al(d, n) reactions, Nucl. Instrum. Methods in Phys. Res. A **652** (2011) 397–399

10) V. Bildstein, P.E. Garrett, J. Wong, et al., Comparison of deuterated and normal liquid scintillators for fast-neutron detection, Nucl. Instrum. Methods in Phys. Res. A **729** (2013)188–197

11) Chris C. Lawrence, Michael Febbraro, Marek Flaska, Sara A. Pozzi, F.D. Becchetti, Warhead verification as inverse problem: Applications of neutron spectrum unfolding from organic-scintillator measurements, J. Appl. Phys.**120** (2016) 064501–1–16.

12) M. Moszynski, et al., Identification of different reaction channels of high energy neutrons in liquid scintillators by the pulse shape discrimination method, Nucl. Instrum. Methods in Phys. Res. A **343** (1994) 563-572

13) Non-Proportionality of Organic Scintillators and BGO, A. Nassalski, M. Moszynski, A. Syntfeld-Ka˙zuch, Ł.S´ widerski, and T. Szcze'sniak, IEEE Trans, Nucl. Sci. **55** (2008) 1069-1072

14) F.D. Becchetti, C.E. Thorn, M.J.Levine, Response of plastic scintillator detectors to heavy ions, $Z \leq 35$, $E \leq 170$ MeV, Nucl. Instrum. Methods **138** (1976) 93-104

15) Haitang Wang, Andreas Enqvist, Pulse height model for deuterated scintillation detectors, Nucl. Instrum. Methods in Phys. Res. A **804** (2015) 167-174

16) Haitang Wang, Donald Carter, Thomas N. Massey, Andreas Enqvist, Neutron light output function and resolution investigation of the deuterated organic liquid scintillator EJ-315, Rad. Meas. **89** (2016) 99-106

17) F.D. Becchetti, R.S. Raymond, R.O. Torres-Isea, A. Di Fulvio, S.D. Clarke, S.A. Pozzi, M. Febbraro, Deuterated -xylene (xylene-d10; EJ301D): A new, improved deuterated liquid scintillator for neutron energy measurements without time-of-flight, Nucl. Instrum. Methods in Phys. Res. A **820** (2016) 112–120

18) A. Di Fulvio, F.D. Becchetti, R.S. Raymond, R.O. Torres-Isea, S.D. Clarke, S.A. Pozzi, Characterization of deuterated-xylene scintillator as a neutron spectrometer, IEEE Trans. Nucl. Sci. **64** (2017) 1825–1832

19) N. Zaitseva, A. Glenn, L. Carman, R. Hatarik, S. Hamel, M. Faust, B. Schabes, N. Cherepy, S. Payne, Pulse shape discrimination in impure and mixed single-crystal organic scintillators IEEE Trans. Nucl. Sci. **58** (2011), 3411-3420

20) M. Febbraro, F.D. Becchetti, R.O. Torres-Isea, J. Riggins, C. C. Lawrence, J.J.Kolata and A.M. Howard, (d,n) proton-transfer reactions on ^{9}Be, ^{11}B, ^{13}C, ^{14,15}N, and ^{19}F and spectroscopic factors at E_d=16 MeV, Phys. Rev. C **96** (2017) 024613.

21) Michael T. Febbraro, *A Deuterated Neutron Detector Array for the Study of Nuclear Reactions with Stable and Rare Isotope Beams*, Ph.D. thesis, The

University of Michigan (Applied Physics, 2014)

22) Christopher C. Lawrence, *Neutron Spectrum Unfolding with Organic Scintillators for Arms-control Verification*, Ph.D. thesis, The University of Michigan (Nucl. Eng. Rad. Sci., 2014)

23) F.D. Becchetti, M. Febbraro, R. Torres-Isea, M. Ojaruega, and L. Baum, ^{252}CF fission-neutron spectrum using a simplified time-of-flight set up: An advanced teaching laboratory experiment , Am. J. Phys. **81** (2013)112-118

24) Kineo Tsukada and Shiroh Kikuchi, Directional asymmetry in the characteristics of organic-crystal scintillators, Nucl. Instrum. and Methods **17** (1962) 286-288

25) S.A. Pozzi, E. Padovani, M. Marseguerra, MCPN-PoliMi: a Monte Carlo code for correlation measurements, Nucl. Instrum. and Methods in Phys. Res. A **513** (2003) 550-558

26) Eljen Technology, Sweetwater, Texas 79556

27) Inrad Optics, Northvale, NJ 07647

28) Joseph S. Carlson, Peter Marleau, Ryan A. Zarkesh, and Patrick L. Feng, J.Am.Chem.Soc. **139** (2017) 9621-9626

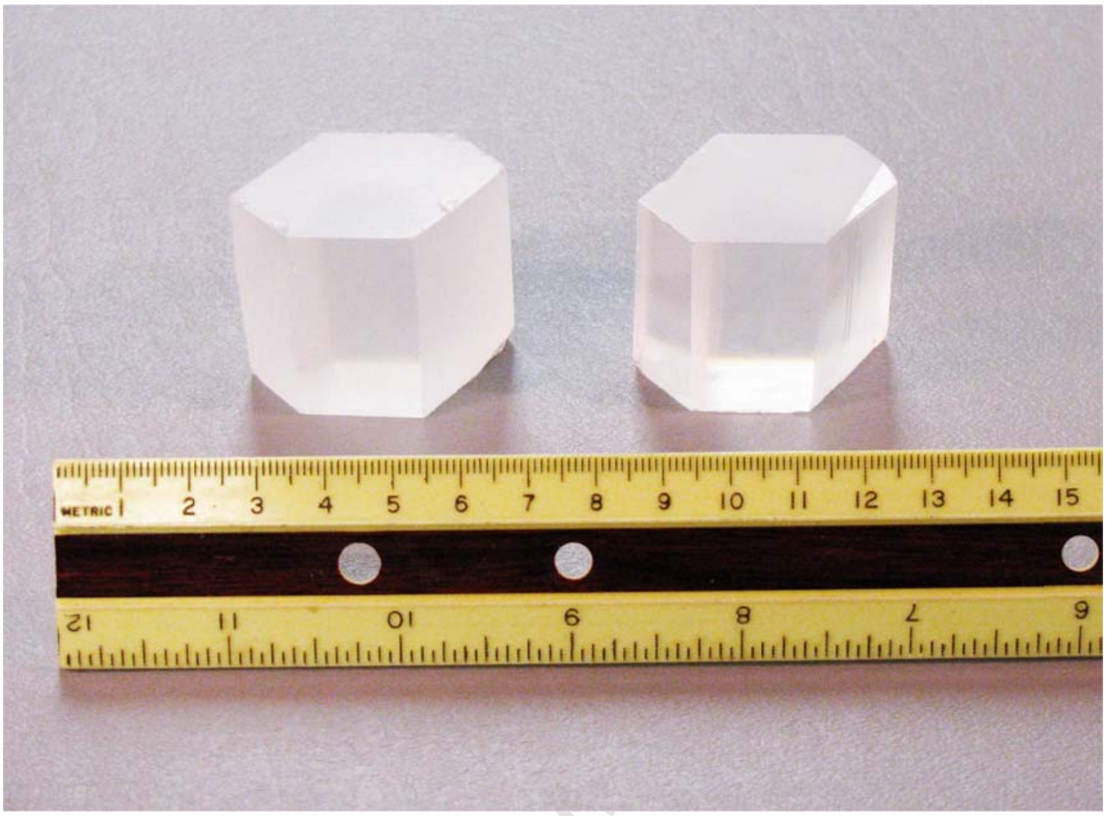

Fig. 1: The large ca. 32 cm^3 LLNL-grown trans-stilbene crystals used for the measurements: Left, stilbene-d_{12}; Right, Similar-size conventional ^{1}H-stilbene crystal.

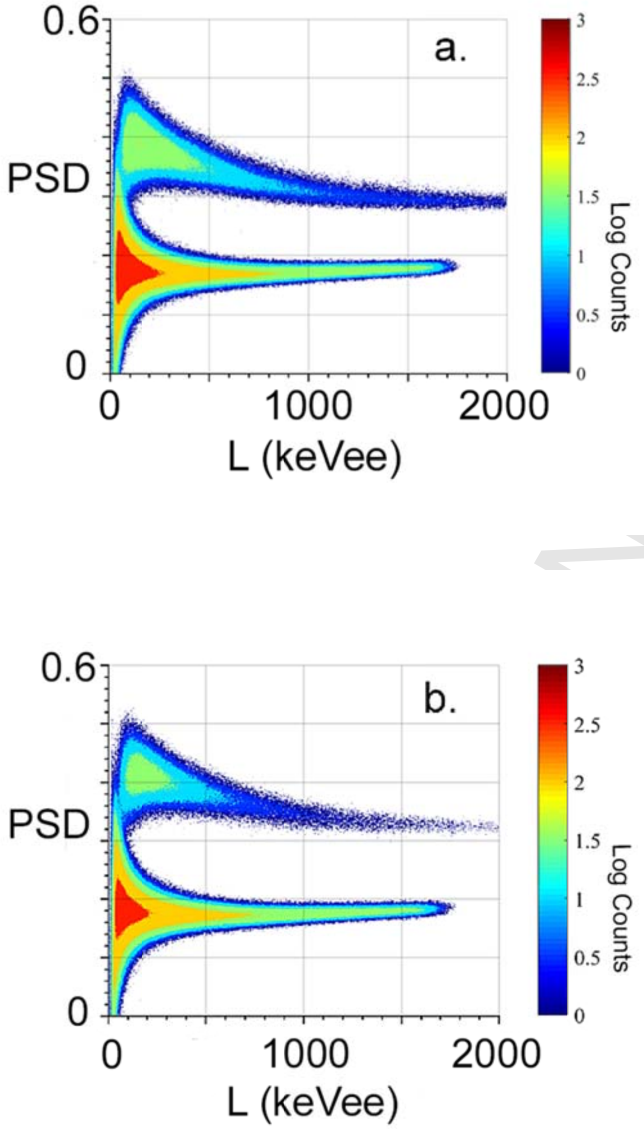

Fig. 2: PSD spectra for a ^{252}Cf source observed in a conventional 32 cm^3 ^1H-stilbene detector (a) compared with the PSD from the matching stilbene-d_{12} detector (b).

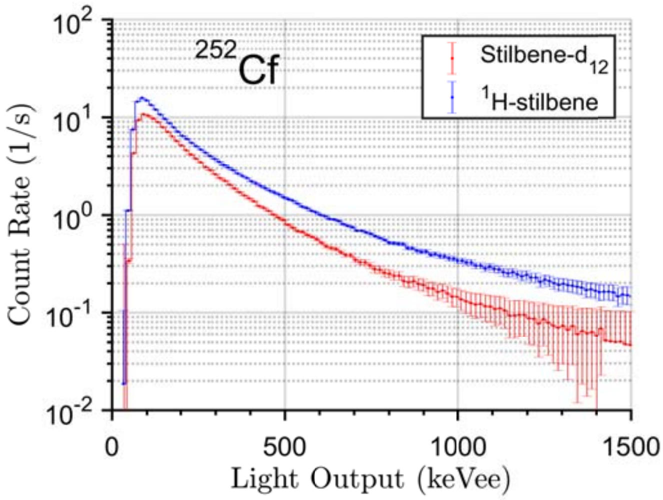

Fig.3: Light spectra for ^{252}Cf fission neutrons obtained using the 32 cm^3 stilbene-d$_{12}$ and conventional ^{1}H-stilbene detectors.

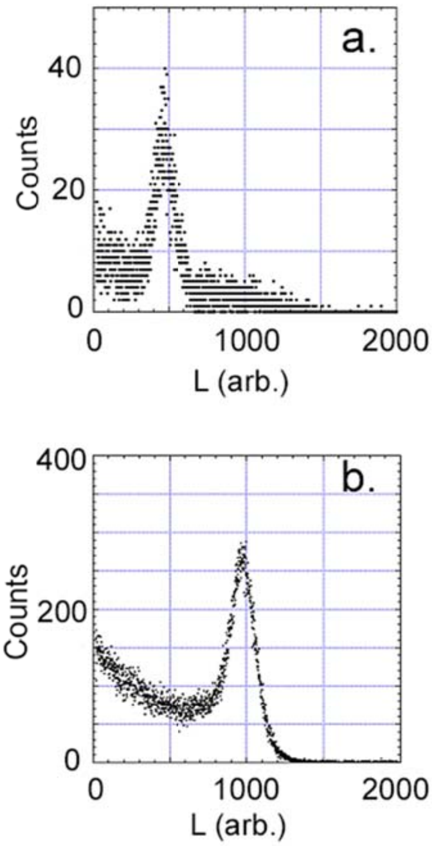

Fig. 4: Light output measured for Compton recoil electrons in the 32 cm^3 stilbene-d$_{12}$ detector from a ^{137}Cs source in coincidence with gamma rays at 60 deg. (a) and 140 deg. (b) in a collimated NaI(Tl) detector.

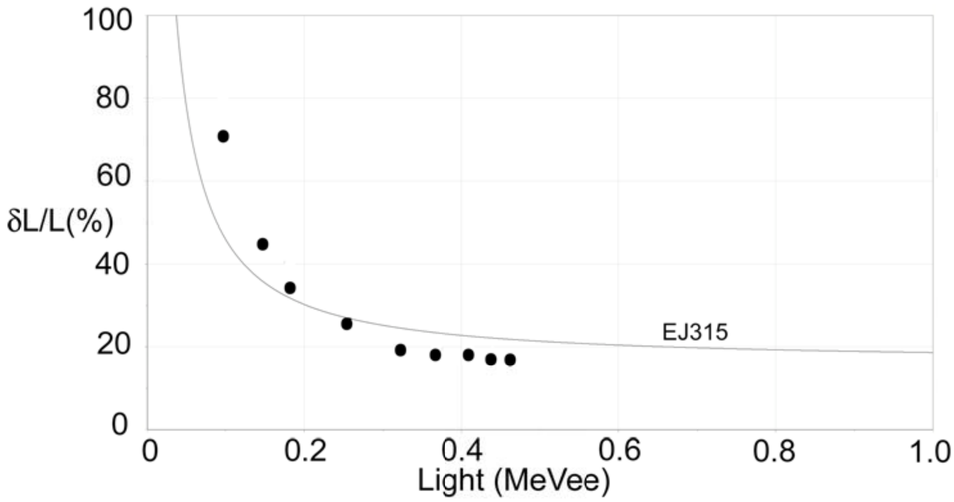

Fig. 5: The resolution of the detector light output measured with Compton recoil electrons (Fig.4) as function of electron energy for the 32 cm^3 stilbene-d_{12} detector (solid circles). The resolution determined for a commercial deuterated-benzene EJ315 detector 7.6 cm dia. by 7.6 cm long as reported in [16] also is indicated.

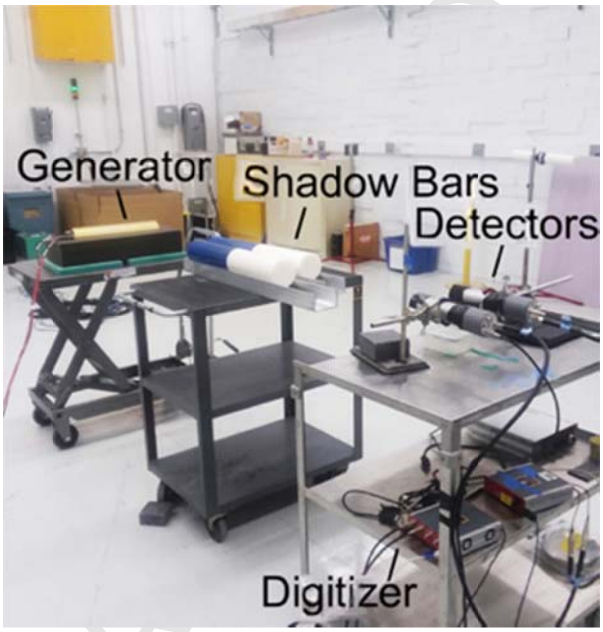

Fig.6: Typical set up with composite shadow bars for measurements with the DD and DT (shown) generators at the UM Neutron Science Lab.

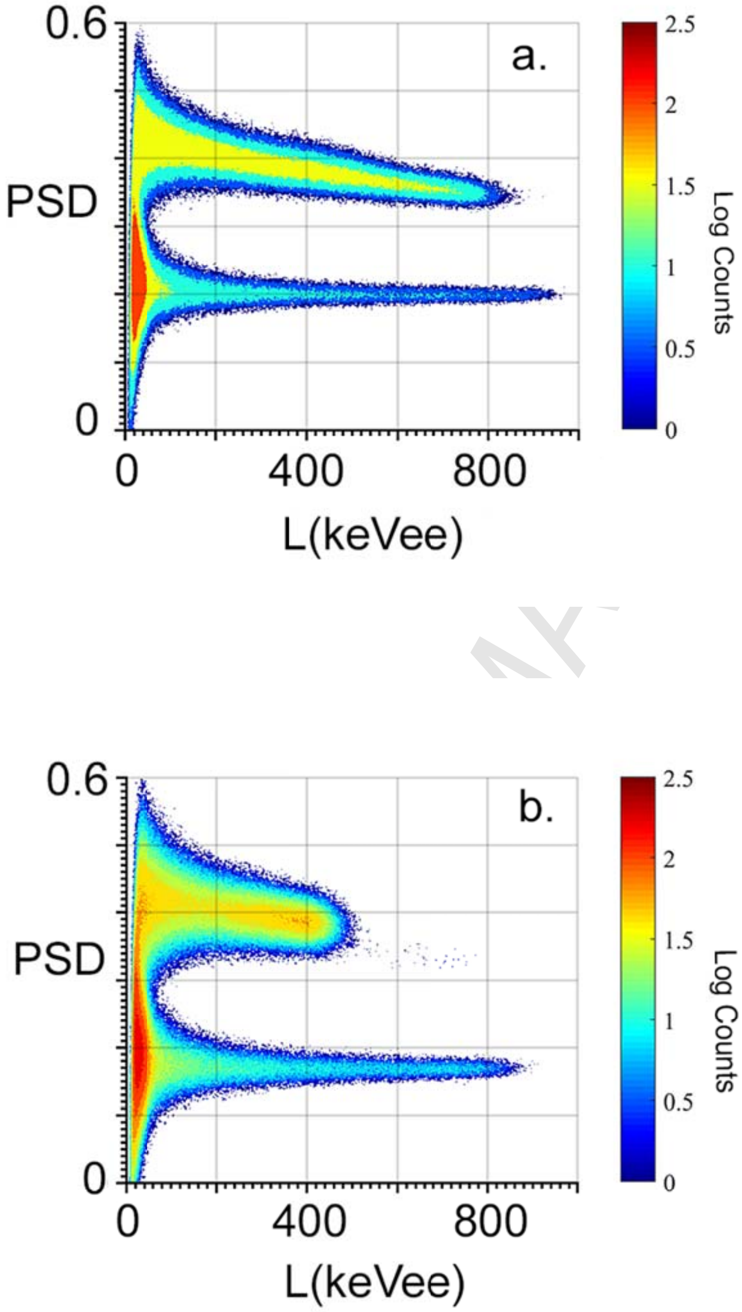

Fig. 7: PSD of the 32 cm^3 stilbene-d_{12} crystal (bottom;b) for DD neutrons (2.5 MeV) compared with the PSD for the similar-size ^{1}H-stilbene detector (top;a). The RH scale represents log counts.

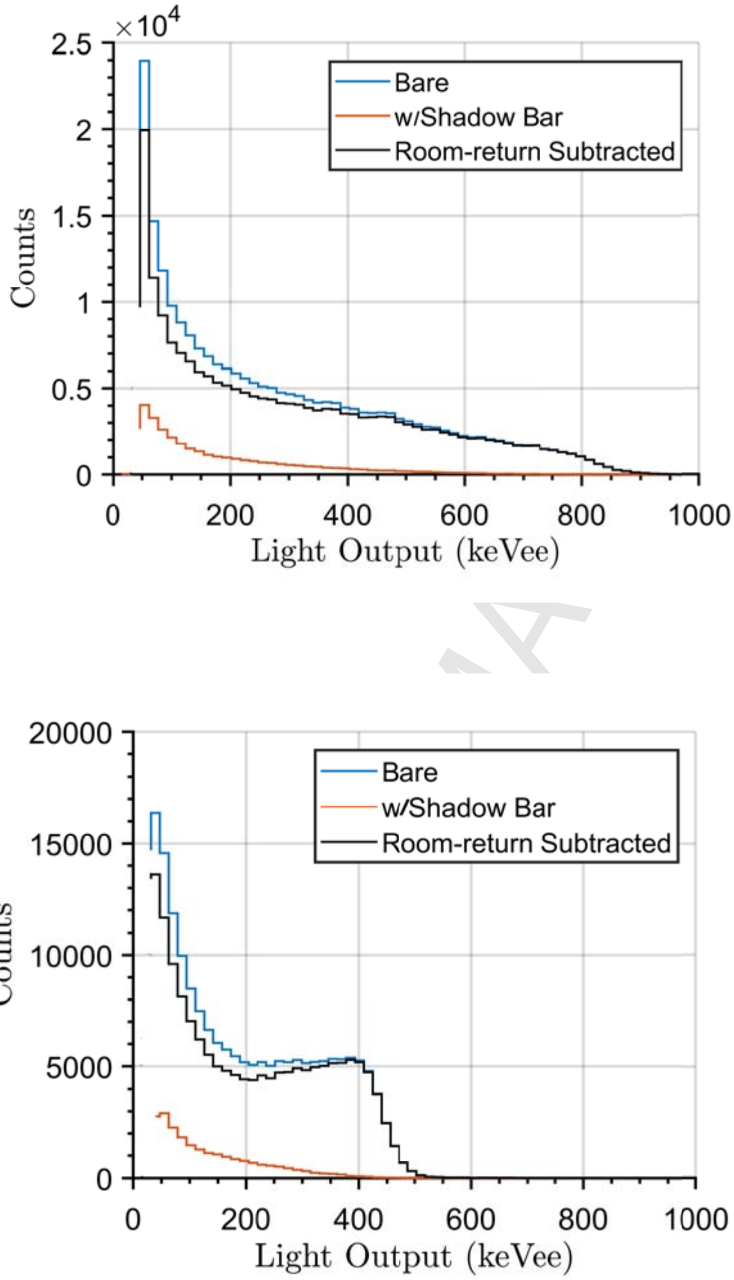

Fig.8: Comparison of light output obtained with the 32 cm^3 stilbene-d_{12} detector (bottom) and the similar-size standard ^{1}H-stilbene detector (top) for PSD-gated DD neutrons (2.5 MeV). Corrections for neutron background using a ca.12 inch steel shadow bar are indicated.

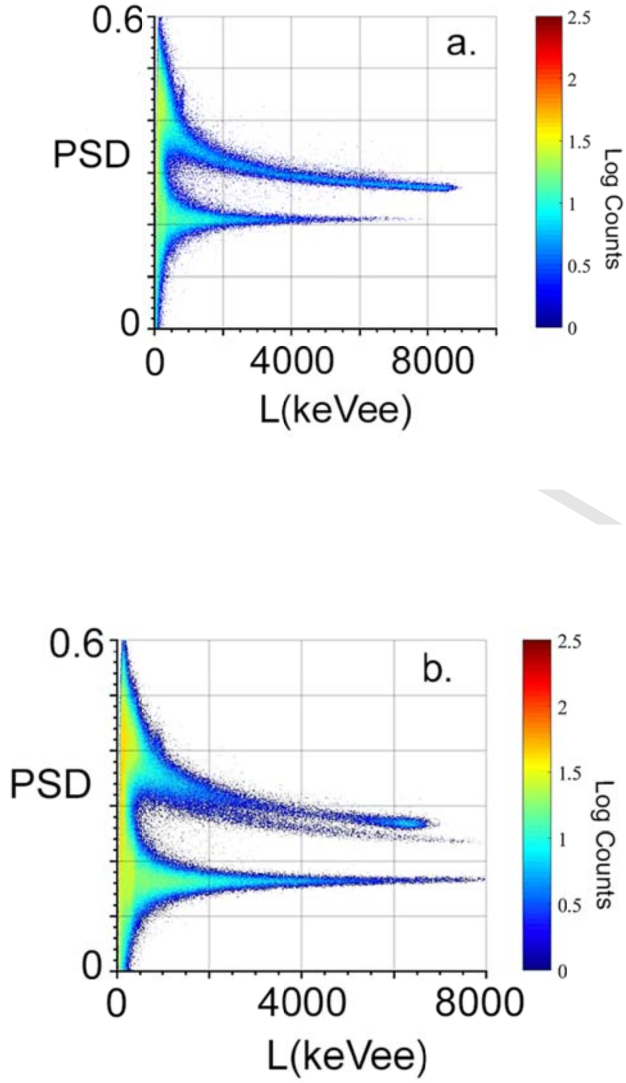

Fig. 9: PSD of the 32 cm^3 stilbene-d_{12} crystal (bottom;b) for DT neutrons (14.1 MeV) compared with the PSD for a similar-size ^{1}H-stilbene detector (top;a). A small contribution due to protons from scintillator-deuteron break up in the stilbene-d_{12} is indicated in the neutron PSD band below the recoil deuterons (see text). The RH scale represents log counts.

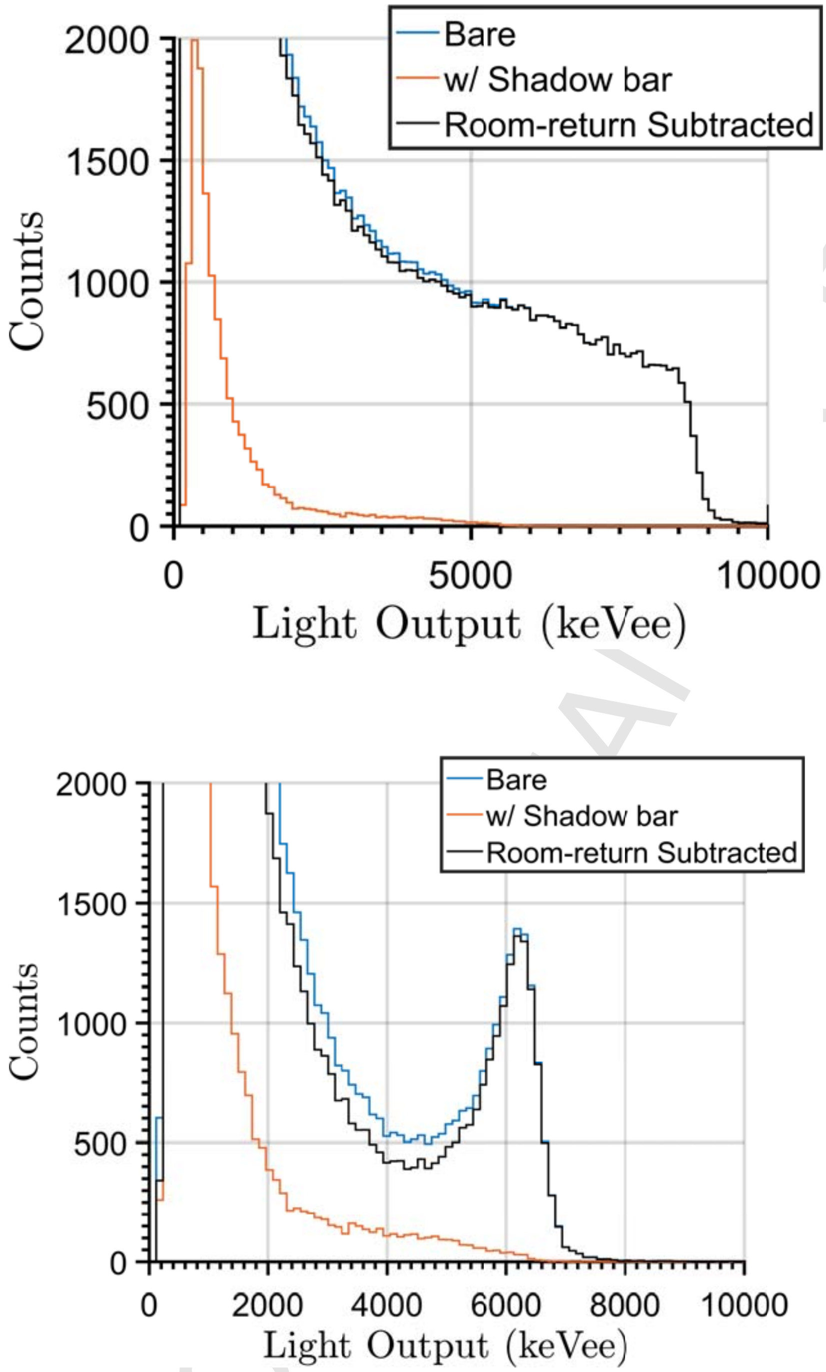

Fig.10: Comparison of light output obtained with the 32 cm^3 stilbene-d_{12} detector (bottom) and the similar-size 1H-stilbene detector (top) for DT neutrons (14.1 MeV). All groups in the neutron PSD band are included in the light spectrum (Fig.9). Corrections for neutron background using composite steel and polyethylene shadow bars (Fig.6) are indicated.

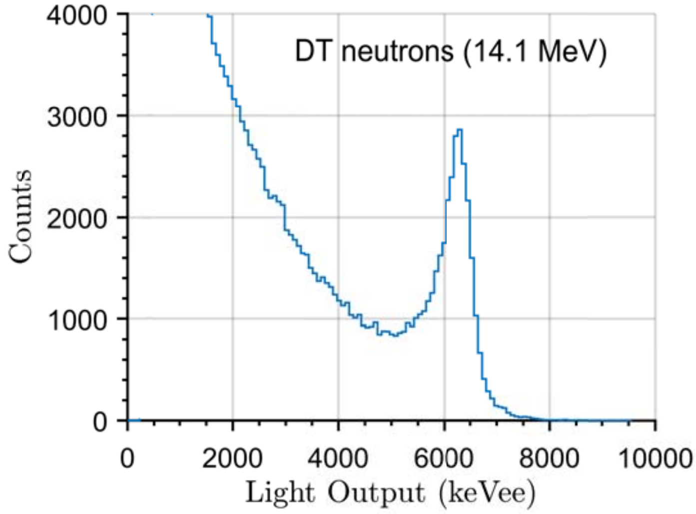

Fig. 11: The resulting high-energy portion of the DT spectrum (background subtracted) for DT neutrons (14.1 MeV) with a 2D gate set to exclude the contribution due to protons from scintillator-deuteron break up in the neutron PSD band (Fig.9).

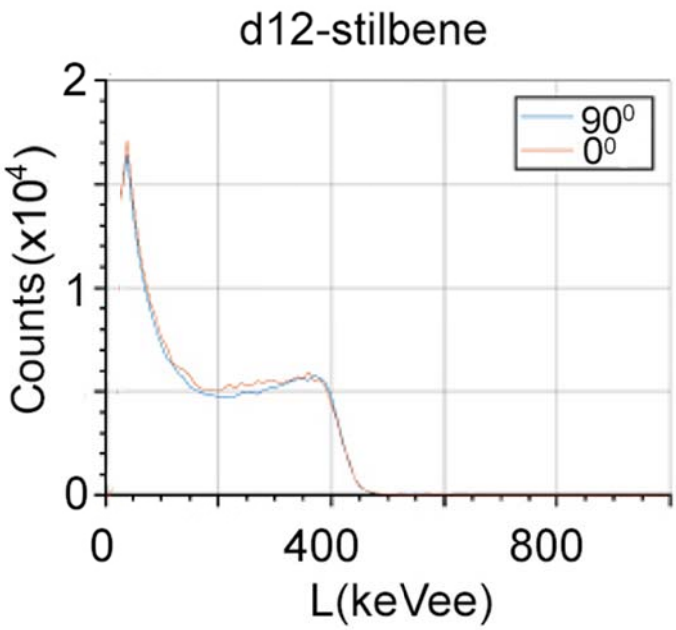

Fig. 12: Tests of asymmetrical response in the small stilbene-d_{12} detector using the DD generator with neutrons incident head on and at 90 degrees to the crystal.